Molecular Crystals and Liquid Crystals
Publication details, including instructions for authors and subscription information:
http://www.tandfonline.com/loi/gmcl20

Linear and Non-Linear Optical Properties of Carbon Nanotubes

S. Lefrant [a], J. P. Buisson [a], J. Y. Mevellec [a], M. Baibarac [b] & I. Baltog [b]

[a] Institut des Matériaux Jean Rouxel, Nantes Cédex, France

[b] National Institute of Materials Physics, Lab. Optics and Spectroscopy, Bucharest, Romania

Version of record first published: 28 May 2010

To cite this article: S. Lefrant, J. P. Buisson, J. Y. Mevellec, M. Baibarac & I. Baltog (2010): Linear and Non-Linear Optical Properties of Carbon Nanotubes, Molecular Crystals and Liquid Crystals, 522:1, 172/[472]-179/[479]

To link to this article: http://dx.doi.org/10.1080/15421401003719910

Mol. Cryst. Liq. Cryst., Vol. 522: pp. 172/[472]–179/[479], 2010

ISSN: 1542-1406 print/1563-5287 online
DOI: 10.1080/15421401003719910

Taylor & Francis
Taylor & Francis Group

Linear and Non-Linear Optical Properties of Carbon Nanotubes

S. LEFRANT,[1] J. P. BUISSON,[1] J. Y. MEVELLEC,[1] M. BAIBARAC,[2] AND I. BALTOG[2]

[1]Institut des Matériaux Jean Rouxel, Nantes Cédex, France
[2]National Institute of Materials Physics, Lab. Optics and Spectroscopy, Bucharest, Romania

Carbon nanotubes are attractive materials with numerous possibilities of applications in various domains. Nevertheless, pertinent characterization studies are required in order to insure reproducibility in preparation, handling and incorporation in devices. Several spectroscopic tools have been developed so far, such as transmission electron microscopy and near-field electrical microscopy. Optical techniques have also been improved with the use of Raman Scattering, Surface Enhanced Raman Scattering (SERS) and near-field optical spectroscopy (SNOM). These non-destructive techniques have been used for nanotubes after synthesis and exploited to follow the modifications of their spectroscopic features when they are functionalized or embedded in host matrices. In this paper, we show that, by using SERS conditions, a new effect is observed: a "single-beam pumped" Coherent anti-Stokes Raman Scattering (CARS). We demonstrate that under a tight–focusing of the excitation light, this emission, resulting from a wave mixing process between the incident laser light (ω_l) and Stokes Raman light (ω_s), is generated by a Surface Enhanced Raman Scattering (SERS) mechanism. Since abnormal anti-Stokes/Stokes intensity ratios are also observed for carbon nanotubes in powders, we have investigated in details their behaviour as a function of several parameters which include the excitation wavelengths, the laser power, the sample support, as well as the presence of nanotubes in isolated or in bundled form. It appears that resonance phenomena explain the anti-Stokes/Stokes intensity ratios in the case of powders and that CARS is only observed when SERS conditions are used. In addition, we have investigated other materials in which anomalies are also observed. This is the case of poly(bithiophene) (PBTh) electrochemically polymerized on carbon nanotubes for which its main Raman line at 1450 cm^{-1} is enhanced, this enhancement being presumably generated by the plasmon excitation of metallic tubes. In the case of PEDOT, the analysis of the anti-Stokes branch provides additional information on the functionalization of carbon nanotubes with this polymer.

Keywords Carbon nanotubes; CARS emission; hybrid carbon nanotube/conjugated polymer materials; Raman scattering

Address correspondence to Prof. S. Lefrant, Institut des Matériaux Jean Rouxel, 2 rue de la Houssinière, B.P. 32229, 44322 Nantes Cédex 03, France. Tel.: +33 240 373 910; Fax: +33 240 373 995; E-mail: Serge.Lefrant@cnrs-imn.fr

1. Introduction

Since their discovery in 1991 by Iijima [1], carbon nanotubes have been extensively studied in particular by using two major techniques, i.e., high resolution Transmission Electron Microscopy (HR-TEM) [1] and Resonant Raman Scattering [2,3]. Since the very beginning, the vibrational modes of carbon nanotubes have been calculated on the basis of the extended knowledge acquired in graphite and/or graphitic compounds [4]. Let us recall that in the particular case of single walled carbon nanotubes (SWNTs), three domains of frequencies are of primary interest: i) in the low frequency range 150–300 cm^{-1}, where the radial breathing modes are observed; ii) the high frequency range, 1400–1700 cm^{-1}, where we find the tangential modes and iii) between 1300 and 1400 cm^{-1} where the so-called "D" band is recorded. The two former domains of frequencies are used to determine the diameter distribution on one side and their electronic structure on the other side, respectively [2,3]. The "D" band is used as a probe for defects in graphite [5] or carbonaceous compounds. It results from a double resonance process as demonstrated in Ref. [6].

Besides the usefulness of resonance Raman scattering as a tool for a good characterization of SWNT samples, several questions remain concerning the environment, since SWNTs can exist in several forms, i.e., isolated or in bundles, functionalized, accommodated in host matrices or in solutions, etc.... This has never been controlled completely and therefore, the quantitative determination of the diameter distribution, as well as the electronic properties of the studied tubes, remain sometimes imprecise. Despite the fact that several attempts have been made to determine the spectroscopic features of isolated tubes [7], data remain dispersed in literature.

Surface Enhanced Raman Scattering (SERS) has also been extensively utilized in several cases to investigate nanotubes, mainly to benefit from a strong signal amplification whenever individual tubes had to be studied [8,9]. However, by using SERS conditions, i.e., by using rough Au or Ag metallic substrates on which samples are deposited, new phenomena have been discovered. For example, in the case of crystal violet (CV) or rhodamin, K. Kneipp and co-workers [9] reported a quadratic behavior for the anti-Stokes signal as a function of the laser power, whereas the Stokes signal follows an usual linear law. This phenomenon was also observed in the case of SWNTs. This was interpreted by an over population of the first excited state induced by spontaneous surface enhanced Raman scattering [9]. But more recently, it was demonstrated that these results may be explained by a new phenomenon, namely a single-pumped coherent anti-Stokes Raman scattering (CARS) mechanism [10]. This was shown by measuring the anti-Stokes Raman band intensities which exhibit abnormal behavior compared to what is expected from the Mawxell-Boltman law, even at high frequencies. This is not restricted to SWNTs. Anomalies have been observed in other compounds such as conjugated polymers deposited on SWNTs used as nano-structured supports. A few examples are described briefly in this paper.

2. Results and Discussion

The CARS-type phenomenon [11] can be observed if the excitation energy coincides with the energy of electronic transitions. This is a requirement for generating non-linear processes since the dielectric susceptibility $\chi^{(3)}$ turns out to be different from zero. CARS is generally described as a four-wave mixing process in which

the anti-Stokes light (ω_{as}) results from the parametric coupling of the incident laser light (ω_l), the Stokes light (ω_s; $\omega_s < \omega_l$) and a probe light (ω_p). if $\omega_l = \omega_p$, the CARS experiments appear as a degenerate four-wave mixing process that reduces to an energy transfer between the two pump waves, ω_l and ω_s which are, in general, supplied by two independent lasers or are generated by parametric frequency conversion. In our case where we use a simple experimental set up under conditions of tight focusing of a single laser excitation beam [10], the second pump wave is achieved by: i) the Surface Enhanced Raman Scattering (SERS) mechanism that supplies the ω_s pump light discretely distributed over all Raman transitions and situated in a broad spectral range and ii) the use of only one laser light with a wide emission band, which passed through a dispersion system – diffraction grating – simultaneously supplying the two pump waves, ω_l and ω_s. In the former case, the SERS mechanism operating over a wide spectral range furnishes ω_s for all Raman lines while in the latter case, ω_s is determined by the spectral width of the exciting light, so that the CARS effect is limited to low-wavenumber vibrational modes situated in the range of 50–400 cm^{-1}.

In the plane-wave approximation and for a non-absorbing medium, the CARS intensity depends on several parameters and non-linearly on the incident pump intensity I_l:

$$I_{CARS} \propto N_A \omega_{as}^2 d^2 |\chi^{(3)}|^2 I_l^2 I_s \, \mathrm{sinc}^2(|\Delta k| d/2) \quad (1)$$

in which $\chi^{(3)}$ is the third order nonlinear dielectric susceptibility, d is the sample slab thickness, sinc(x) means sin(x)/x and N_A is the numerical aperture of the collecting lens. The coherent nature of the CARS process is reflected by fulfilling the phase-matching condition $|\Delta k| \cdot d \ll \pi$ where $\Delta k = k_{as} - (2k_p - k_s)$ and k_{as}, k_s and k_p are the wave vectors of the anti-Stokes, Stokes and pump light, respectively. For condensed media, if the beams cross at an angle θ, the small dispersion of refractive index makes $\Delta k \approx 0$ over small paths. For tightly focused beams, the requirement of phase matching relaxes, being no longer sensitive to the Raman shift and so a CARS spectrum can be observed at an angle θ_{as} larger than the Stokes angle θ_s . Therefore, the challenge is to demonstrate that at resonant laser excitations, when the excitation light coincides with an electronically allowed transition ($\chi^{(3)} \neq 0$), the intensity of the anti-Stokes emission is enhanced according to Eq. (1).

The quadratic dependence of the anti-Stokes spectra intensity on the SWNTs film thickness has been reported several times [9,10]. The abnormal anti-Stokes Raman emission was measured by the ratio I_{aS}/I_S, at $\lambda_{exc} = 676.4$ and 514.5 nm for the G band. We found values of 0.5 and 0.02 which are much larger than $2 \cdot 10^{-5}$ resulting from calculations. The asymmetric G band profile appearing at 676.4 nm exciting laser light indicates the strong resonant excitation of metallic nanotubes also noted by a higher value of the ratio I_{aS}/I_S.

Figure 1 discloses Raman spectra of SWNTs, recorded under similar conditions, at an excitation of 676.4 nm on two types of substrates, an Au surface used as a SERS support (Fig. 1a) and a porous Si substrate (Fig. 1b). In Figure 1b, we have also reported the anti-Stokes intensity calculated from the Stokes branch by using the Maxwell-Boltzman law. Experimentally, these data confirm, as expected, that for SWNTs film deposited on a porous silicon support, we are unable to produce a SERS enhancement. Other parameters expressed in Eq. (1) for the CARS intensity, like the film thickness, the numerical aperture of the microscope used to record

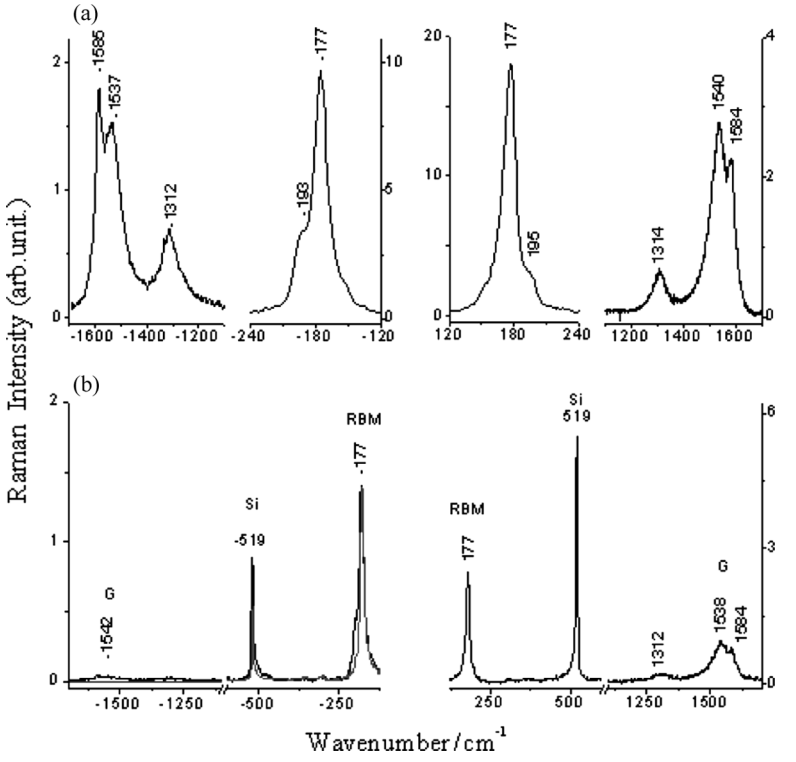

Figure 1. Anti-Stokes and Stokes SERS spectra on SWNT films, $\lambda_{exc} = 676.4$ nm: (a) on a rough Au support; (b) on a porous Si support.

micro-Raman spectra, the laser power, have been shown to be in agreement with the CARS phenomenon, as reported elsewhere [10].

In the case of SWNTs in powders, differences in anti-Stokes/Stokes ratios have been also observed, especially for radial breathing modes. An example in this sense was reported in Ref. [12]. The radial breathing modes recorded at 161 and 177 cm^{-1} for an excitation $\lambda_{exc} = 1064$ nm exhibit Anti-Stokes/stokes ratios significantly different since they are 0.34 and 1.04 for these modes, respectively. Previous experiments [13] have qualitatively demonstrated that the mode at 161 cm^{-1} could be associated to isolated tubes whereas the one at 177 cm^{-1} to bundled tubes. Therefore this phenomenon was thought to be used to identify isolated tubes from bundles of tubes, keeping in mind that this is not in contradiction with predictions issued from the Kataura plot [14]. Nevertheless, this interpretation does not take into account the double resonance effects which occurs in Raman scattering when the excitation wavelength is changed and which monitor the scattering intensity. This was published several times and described in the following formula [15]:

$$I(E_1) = \int \left| \frac{Mg(E)}{(E_1 - E - i\Gamma_r)(E_1 \pm E_{ph} - E - i\Gamma_r)} \right|^2 dE \qquad (2)$$

In order to investigate these effects, we performed systematic Raman studies on different types of SWNTs (precisely Hipco and arc electric samples) as a function of

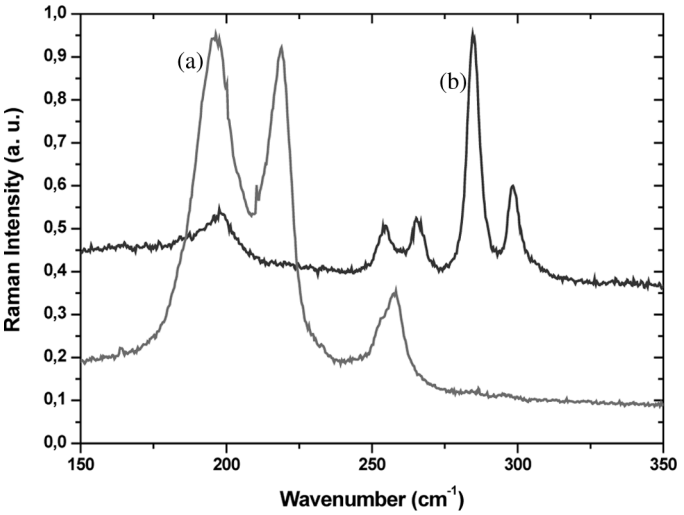

Figure 2. Radial breathing modes recorded at $\lambda_{exc} = 647$ nm: (a) powder; (b) dispersed using a surfactant (SDS).

several parameters including first the excitation wavelength, but also, the temperature induced by the laser power, the environment, etc. Such experiments demonstrate clearly, as expected, that resonance effects can account for strong discrepancies in the antiStokes/Stokes ratios measured on selected RBM frequencies.

In the following, we give two examples illustrated by Figures 2 and 3.

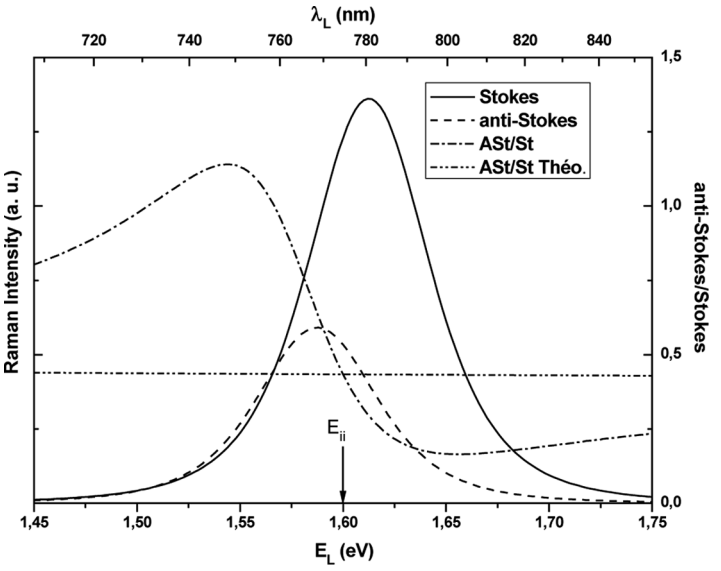

Figure 3. Calculation of the Stokes and anti-Stokes intensities for a RBM at 200 cm^{-1} with an E_{ii} transition energy of 1.60 eV. The anti-Stokes/Stokes ratio is also indicated and the theoretical law is given for comparison.

Figure 2 shows the radial breathing modes of Hipco samples recorded at $\lambda_{exc} = 647\,nm$ in the low frequency range in powder on one hand (red curve) with peaks at 195 and 216 cm^{-1}, and separated from each other by using a surfactant (here SDS). Despite the fact that similar observation conditions are used and that we deal with the same sample, one observes clearly that different modes are observed as a consequence of drastic changes in resonance conditions.

A modelling of the antiStokes/Stokes Raman line intensities, together with their ratios, is illustrated in Figure 3, as a function of the excitation wavelength. We have chosen a nanotube characterized by a RBM at 200 cm^{-1} with a Van Hove transition energy E_{ii} at 1.60 eV. We can obviously observe that the maximum of the Stokes peak is shifted compared to the maximum of the anti-Stokes counterpart. The ratio varies in a large range and in any case does not follow the Maxwell-Boltzman law indicated on the figure for comparison. Therefore, one can conclude that in this case when SERS conditions are not used, the anomalies of the anti-Stokes/Stokes ratios cannot be associated with CARS-type effects and can be presumably explained by changes in resonance conditions induced by several factors as mentioned above.

It remains that CARS-type effects can also be observed in other nanostructures, for example in materials containing conjugated polymers. First, we have demonstrated that in the case of poly-bithiophene deposited on a SWNT thin film, an intense Raman line at 1450 cm^{-1} associated with this polymer is observed in the anti-Stokes branch. This was interpreted by a resonant excitation of plasmons in

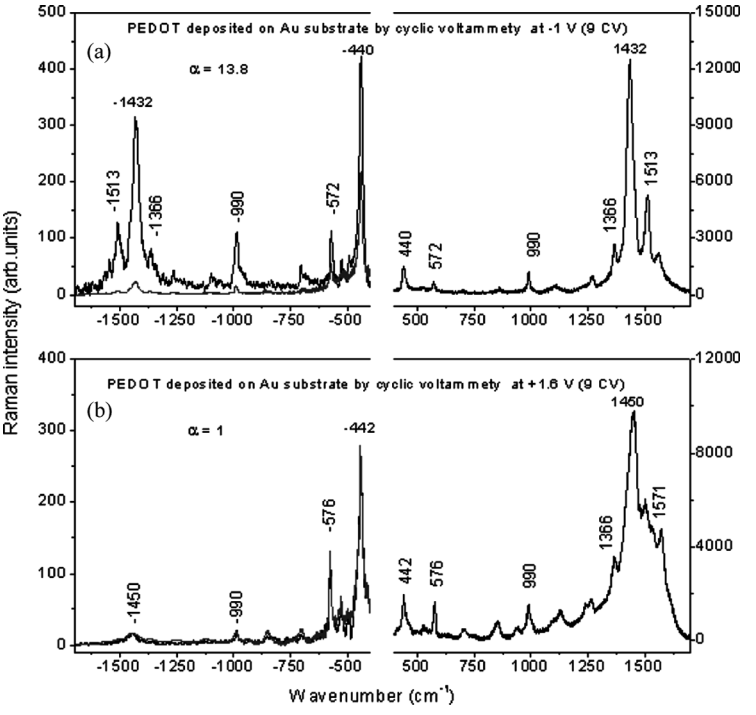

Figure 4. Anti-Stokes and Stokes Raman spectra of PEDOT at $\lambda_{exc} = 514.5\,nm$: (a) neutral form; (b) doped form. The grey curve in the anti-Stokes branch is calculated from the Maxwell-Boltzman formula from the Stokes branch.

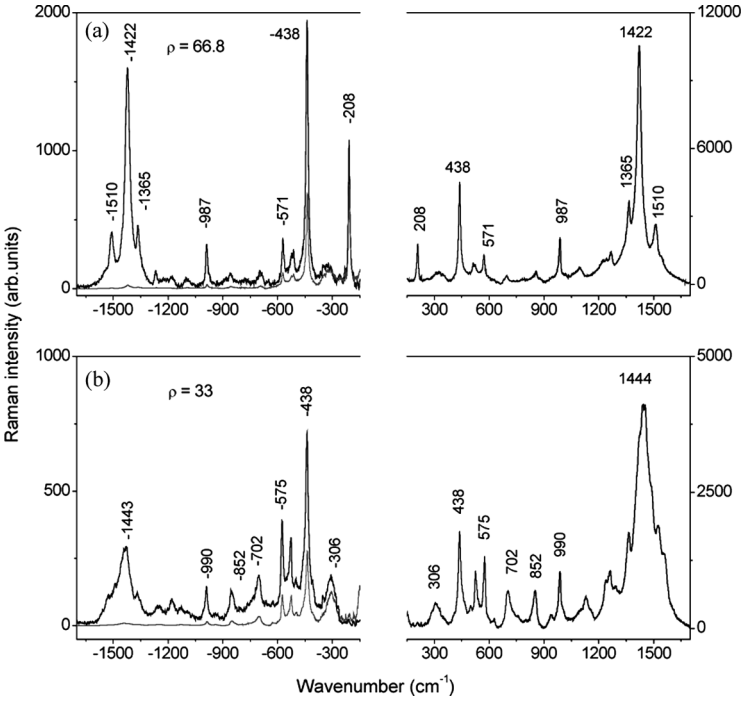

Figure 5. Anti-Stokes and Stokes Raman spectra of PEDOT at $\lambda_{exc} = 676.4$ nm: (a) neutral form; (b) doped form. The grey curves in the anti-Stokes branch are calculated from the Maxwell-Boltzman formula from the Stokes branch.

metallic nanotubes, contributing in an extra way to the anti-Stokes Raman emission having the characteristics of a CARS process [16]. More recently, detailed experiments carried out with PEDOT showed also that the abnormal anti-Stokes Raman effects can be exploited to gain information to evaluate the functionalization of carbon nanotubes with conjugated polymers. In order to do this, we used two different excitation wavelengths, 514.5 nm and 676.4 nm. The 514.5 nm ensures the resonant excitation of undoped PEDOT only, whereas 676.4 nm ensures resonance conditions for doped PEDOT. This is illustrated in Figs. 4 and 5, showing that the anti-Stokes signal is enhanced only when resonance conditions are achieved (un-doped PEDOT, Fig. 4a) whereas no enhancement occurs in the anti-Stokes branch of doped PEDOT (Fig. 4b). On the other hand, for 676.4 nm, both SWNTs and doped PEDOT are resonantly enhanced, as a proof of the CARS-type phenomenon which requires $\chi^{(3)}$ to be different from zero at the excitation wavelength.

4. Conclusions

In this paper, we have shown that a CARS-type effect can be induced in nanostructures such as carbon nanotubes, revealed by antiStokes/Stokes ratios of Raman bands abnormally enhanced. We have demonstrated that SERS conditions are required, since in SWNT powder in which such ratios can also have high values, resonance conditions can explain by themselves experimental data. We have shown also that such results can be exploited fruitfully in a number of other nanostructures

such as hybrid materials combining SWNTs and conjugated polymers. One can probe in such a way functionalization processes and/or simply determine the Raman features of fluorescent polymers by investigating the anti-Stokes branch even at large frequencies, which usually unavailable due to a too low scattering intensity.

Acknowledgments

This work was performed in the frame of the Scientific Cooperation between the the Institute of Materials Jean Rouxel in Nantes, and the Laboratory of Optics and Spectroscopy of the National Institute of Materials Physics, Bucharest.

References

[1] Iijima, S. (1991). *Nature*, *354*, 56.
[2] Dresselhaus, M. S., Dresselhaus, G., Jorio, A., Souza Filho, A. G., & Saito, R. (2002). *Carbon*, *42*, 2043 and references therein.
[3] Dresselhaus, M. S., Dresselhaus, G., Saito, R., & Jorio, A. (2005). *Physics Reports*, *409*, 47 and references therein.
[4] Bandow, S., Asaka, S., Saito, Y., Rao, A. M., Grigorian, l., Richter, E., & Eklund, P. C. (1998). *Phys. Rev. Lett.*, *80*, 3779.
[5] Tuinstra, F. & Koenig, J. L. (1970). *J. Chem. Phys.*, *53*, n°3, 1126.
[6] Thomsen, C. & Reich, S. (2000). *Phys. Rev. Lett.*, *85*, 5214.
[7] Jorio, A., Saito, R., Hafner, J. H., Lieber, C. M., Hunter, M., McClure, T., Dresselhaus, G., & Dresselhaus, M. S. (2001). *Phys. Rev. Lett.*, *86*, 1118.
[8] Lefrant, S., Baltog, I., Lamy de la Chapelle, M., Baibarac, M., Louarn, G., Journet, C., & Bernier, P. (1999). *Synth. Met.*, *100*, 13.
[9] Kneipp, K., Wang, Y., Kneipp, H., Itzkan, I., Dasari, R. R., & Feld, M. S. (1996). *Phys. Rev. Lett.*, *76*, 244.
[10] Baltog, I., Baibarac, M., & Lefrant, S. (2008). *Physica E*, *40*, 2380.
[11] Hayazawa, N., Ichimura, T., Hashimoto, M., Inouye, Y., & Kawata, S. (2004). *J. Appl. Phys.*, *95*, n°5, 2676.
[12] Lefrant, S., Buisson, J. P., Mevellec, J. Y., Baltog, I., & Baibarac, M. (2008). *Phys. Stat. Solidi (b)*, *245*, 2221.
[13] Marcoux, P. R., Schreiber, J., Batail, P., Lefrant, S., Renouard, J., Jacob, G., Albertini, D., & Mevellec, J. Y. (2002). *Phys. Chem. Chem.Phys.*, *4*, 2278.
[14] Kataura, H., Kumazawa, Y., Maniwa, Y., Umczu, I., Suzuki, S., Ohtsuka, Y., & Achiba, Y. (1999). *Synth. Met.*, *103*, 2555.
[15] See for example, Dresselhaus, M. S., Dresselhaus, G., Jorio, A., Souza Filho, A. G., & Saito, R. (2002). *Carbon*, *40*, 2061.
[16] Baibarac, M., Baltog, I., & Lefrant, S. (2009). *Carbon*, *47*, n°5, 1389.